

# Synthesis and Characterization of Xerogel from Palm Kernel Shell Biochar

Nor Mohd Razif Noraini<sup>1,2</sup>, Azil Bahari Alias<sup>\*1</sup>, Deana Qarizada<sup>1,3</sup>, Farah Aida Md Azman<sup>1</sup>, Zulkifli Abdul Rashid<sup>1</sup>, Mohd Rosdi Che Hasan<sup>4</sup>  
<sup>\*</sup>azilbahari@uitm.edu.my

<sup>1</sup>Industrial Process Reliability & Sustainability (INPRES) Research Group, School of Chemical Engineering, College of Engineering, Universiti Teknologi MARA, 40450 Shah Alam, Selangor, Malaysia

<sup>2</sup>National Institute of Occupational Safety & Health (NIOSH), Lot 1, Jalan 15/1, Section 15, 43650 Bandar Baru Bangi, Selangor, Malaysia

<sup>3</sup>Faculty of Chemical Engineering, Jawzjan University, Jawzjan, Afghanistan

<sup>4</sup>One Gasmaster Sdn Bhd, 18, Jalan PJU 3/48, Sunway Damansara Technology Park, 47810 Petaling Jaya, Selangor, Malaysia

## ABSTRACT

*With an alarming amount of agricultural waste disposal rate, it emerges the search to utilize biomass and turn them into a beneficial product. Biochar is one the beneficial product that contains high carbonaceous material that is commonly utilized as an adsorbent. This research aims to characterize and produce xerogel from Palm Kernel Shell (PKS) biochar. The production of Biochar Xerogel was produced through the sol-gel method and further dried in an oven to produce xerogel. The synthesized xerogel was characterized using different characterization techniques which are Fourier Transform Infrared Spectroscopy (FTIR), Brunauer-Emmett and Teller (BET), Scanned Electron Microscopy (SEM) analysis, Thermogravimetric analysis (TGA) and X-Ray Diffraction (XRD). The FTIR spectrum analysis has shown the existence of various functional groups such as hydroxyl, aldehyde, alkane and aromatic groups. The TGA analysis reveals the maximum thermal of 1000 °C for xerogel and XRD patterns reveal the amorphous nature of the extracted xerogel biochar. The BET isotherm revealed xerogel as microporous material with a pore width of 1.5 nm. Meanwhile, the SEM image also shows that the xerogel*

has an apparent pore and the pore size is varied which can function as a good adsorbent.

**Keywords:** Xerogel, Palm Kernel Shell Biochar, Biomass, Characterization, Adsorbent

## Introduction

Biomass has been used as a substitute for traditional materials to manage waste and it's the potential to derive an environmental-friendly adsorbent to reduce pollution. Biomass is defined as a renewable resource that is derived from plant-based material or animal sources [1]. In Malaysia, the palm oil industry is one of the largest contributors to biomass production which includes palm fibre (PF), palm kernel (PK), Empty Fruit Bunch (EFB), and palm oil mill effluent (POME) [2]. The overwhelming amount of biomass production has been brought to attention due to its high disposal rate. Therefore, many researchers have studied the potential of transforming biomass into a beneficial product such as biochar. Biochar has high carbon content and a large surface area which makes it a good adsorbent. However, for maximal potential as an adsorbent, an extremely porous material is required [3]. Therefore, many studies reported that transforming biochar into an organic gel via the sol-gel method has greater adsorption capacity [4]. Different methods of drying organic hydrogels can result in various classifications of gels such as xerogel, cryogel and aerogel when dried under each specified condition [5]. Table 1 shows the drying method and properties of different classifications of gels.

Table 1: Comparison of drying method and porosity for different types of gel

Type of gel	Aerogel	Cryogel	Xerogel
Drying method	Supercritical CO <sub>2</sub> drying	Freeze drying at sub-zero	Oven drying at 60 °C
Porosity (%)	95.1 ± 0.2	94.4 ± 0.3	29.5 ± 1.4

Based on Table 1, the drying methods for xerogel, cryogel and aerogel are subcritical drying, freeze-drying and supercritical drying conditions, respectively [6]. Conventional hydrogels are usually the precursor for the preparation of classified gels. Hydrogels are commonly known for their hydrophilic properties where they can adsorb water without dissolving due to their soft and high capacity of water adsorption [7]. In the previous research, conventional hydrogels are extensively utilized as adsorbents. However, due to their small pore size, poor mechanical qualities, and limited molecular transport, their application has drawbacks. Xerogels have recently been used

as adsorbents for efficient separation and purification because of their high surface area and permeability [8]. Different types of gel depict different properties and adsorption capacities. The hydrogel is commonly evaporated at sub-critical conditions to produce xerogel. Sub-critical drying can be done in a variety of ways, including evaporation, convection, microwave, or vacuum drying, and it is done at ambient temperature. The ambient temperature and pressure can lower the cost of preparation for xerogel. Based on existing research, not many covers the conversion of biochar adsorbents. On the contrary, researchers found that adsorbents are widely produced from activated carbon due to their high adsorption capacity and reusability. However, carbon xerogels are expensive and new material from biomass waste can replace activated carbon. According to [9], due to the high cost of other adsorbents, in search for new materials for adsorbents increased over the years. Comparatively, the production of biochar is cheaper, with lower energy requirements. The palm kernel shell which can be converted to biochar is one of the mentioned bio-wastes that can produce xerogel.

In this study, there are two goals. Firstly, it is to synthesize the biochar xerogel from palm kernel shell biochar. Then, to characterize the morphology and properties of the synthesized xerogel by using different characterization techniques. Each adsorbent depicts a unique shape, density, internal pore surface area, and pore size distribution to execute the best adsorption process possible. Hence, it is critical to understand the correlation between morphology development during processing and material final properties. In the synthesis of xerogel biochar production from palm kernel shell (PKS) biochar, the sol-gel method was applied. To obtain xerogel, the liquid of agitated hydrogel biochar was placed at sub-critical conditions as a drying method. After obtaining the synthesized xerogel biochar, the characterization of xerogel to determine the structural and chemical characteristics whereas identified by different techniques which are Fourier transform infrared spectroscopy (FTIR) analysis for chemical structure measurement, Scanned Electron Microscopy (SEM) analysis for morphological characteristics, Thermogravimetric analysis (TGA) to determine thermal stability, X-Ray Diffraction (XRD) to determine crystalline phases and Brunauer, Emmett and Teller (BET) technique to find out the specific surface area and pore volume.

## **Methodology**

### **Material**

The palm kernel shell (PKS) has been chosen as the organic precursor. A carbon-based organic material will be a commercialized palm kernel shell (PKS) biochar obtained from Eureka Synergy Sdn. Bhd. Activated Carbon

(AC) was obtained commercially. Other chemicals that are required in the synthesis of xerogel biochar are Sodium Alginate as polymer, precipitated Calcium Carbonate as cross-linker and Glucono Delta-Lactone as initiator supplied by Chemiz Malaysia, System Chemicals and Alfa Aesar, respectively. Distilled water was used to prepare the alginate solution throughout the whole experiment.

### Synthesis of xerogel

The schematic diagram for the sol-gel method is shown in Figure 1. The synthesis of xerogel biochar is done by the sol-gel method which includes three main steps: sol-gel formation, aging of gel and drying of gel [10]. In the sol-gel formation section, 8.26 g of Sodium Alginate is completely dissolved in 1000 mL of distilled water to create an alginate solution. According to [11], the concentration of alginate in the solution should achieve 2 wt.%. The alginate solution is prepared 24 h prior to the sample preparation. This step is important to reduce the time of dissolving sodium alginate in distilled water.

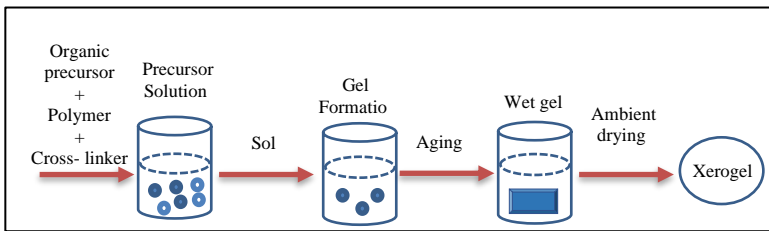


Figure 1: Schematic diagram for Sol-gel

In the sol-gel formation section, 8.26 g of Sodium Alginate is completely dissolved in 1000 mL of distilled water to create an alginate solution. According to [12], the concentration of alginate in the solution should achieve 2 wt.%. The alginate solution is prepared 24 hr prior to the sample preparation. This step is important to reduce the time of dissolving sodium alginate in distilled water. Then, 5.75 g of PKS biochar and 3.46 g of Calcium Carbonate powder were added to the alginate solution. With a vigorous mixing of the solution at 450 rpm on a hot plate, a colloidal suspension (sol) results through a hydrolysis and condensation process. The colloidal suspension (sol) is then converted into a gel by crosslinking Calcium Carbonate ( $\text{CaCO}_3$ ) through the polymerization process. In addition, 9 g of Glucono Delta-Lactone (GDL) was added into the alginate/ $\text{CaCO}_3$  mixture solution when it is homogenous to initiate the ionization of  $\text{CaCO}_3$ . Glucono Delta-Lactone hydrolyzes (GDL) into gluconic acid, which allows the dissolution of calcium carbonate and alginate particles [23]. The importance of adding calcium carbonate to the alginate solution is to allow calcium ions ( $\text{Ca}^+$ ) in the solution

to cross-link with alginate polymers. The cross-linking process will result in a gel. Figure 2 shows the ionic cross-linking of an alginate solution.

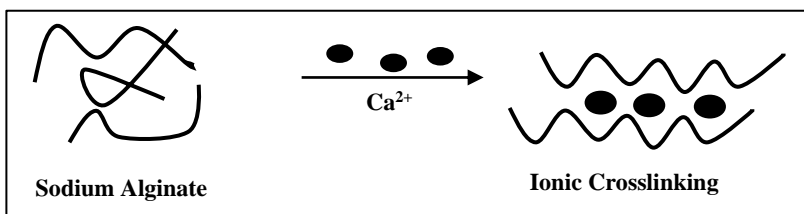


Figure 2: Ionic cross-linking of an alginate solution resulting in alginate gel formation with characteristic egg-box calcium-linked junctions

In Figure 2, the sodium (alginate counter ions) encounters an ion exchange with the multivalent cations to form gelation of alginates. The multivalent cations allow the G blocks in the alginate polymer to be stacked to produce the distinctive "egg box." Calcium carbonate, which is calcium salt, is mixed with the alginate solution because of its water-insoluble properties. With that, calcium ions are then released from the interior of the alginate phase by the dissolution of calcium carbonate with an acid [13]. To ensure complete polymerization and cross-linking reaction, the aging process is done by keeping the formed gel for a few hours to several days at an ambient temperature until a stable wet gel is formed. Then, the blended wet gel biochar is taken and poured into a silicone mold to achieve the desired size. After that, the small-sized gel biochar was washed repeatedly to allow the removal of any unwanted monomers. In previous studies, there are various opinions on the temperature of the oven drying to obtain the final xerogel. A study report by [14] found that the wet gels were dried at 60 °C for 3 hours to obtain the final xerogel sample. Figure 3 shows the synthesized xerogel biochar.



Figure 3: Extracted xerogel biochar

As for the research experiment, the wet xerogel was dried in an oven at 80 °C for 24–72 hours for a complete dry. After the xerogel was completely dried, it was crushed into fine powder to prepare for characterization analysis.

## **Characterization of Xerogel**

### **Fourier transform infrared spectroscopy (FTIR)**

The chemical structure of the synthesized xerogel was measured using a Bruker FTIR spectrophotometer by following the ASTM standard test method (E1252-98). The practice covers a spectral range of 4000–450  $\text{cm}^{-1}$  according to the ASTM E1252-98. The chemical structure including the functional group of the xerogel was analysed. The synthesized xerogel biochar was crushed to form a fine powder. In research done by [14], the FTIR spectra were used at a range of 4000–450  $\text{cm}^{-1}$ . The carbon samples of xerogel and palm kernel shell (PKS) biochar were analyzed simultaneously for comparison. The spectrogram was observed on the computer monitor where a graphic representation of the sample spectrogram was portrayed.

### **Thermogravimetric analysis (TGA)**

To estimate the element content such as moisture content, volatile matter content, carbon content and maximum temperature profile of synthesized xerogel, the thermogravimetric (TG) method was used by using the Mettler Toledo Thermogravimetric Analyzer [7]. Thermogravimetric analysis is done to study the stability of the extracted xerogel following ASTM standard method D5142-02a. The xerogel biochar and palm kernel shell (PKS) biochar samples were heated up to 950 °C with a heating rate of 20 °C/min in the presence of air involving a nitrogen atmosphere at 100 ml/min flow rate of gas. Then, the sample atmosphere is switched into the air and heated up to 1200 °C.

### **X-Ray diffraction analysis (XRD)**

To analyze the structure of materials from the scattering pattern produced by a beam of x-ray interacting with the particle. This is then matched to an existing database to determine the chemical components within the material. The x-ray diffraction analysis was done by using the XRD diffractometer system (RIGAKU) with the diffraction of  $2\theta$  at values ranging from 10 to 90°. In the broad XRD array of extracted silica at  $\theta = 22.5^\circ$ , a distinctive amorphous solid is observed which confirms the formation of amorphous silica phase identification. According to [4], the typical diffraction of amorphous silica ( $\text{SiO}_2$ ) xerogel is a broad peak at  $2\theta = 22^\circ$ .

### **Brunauer-emmett and teller (BET)**

To find out the specific surface area, pore volume, and pore size distribution, Brunauer-Emmet Teller (BET) theory was used. For this analysis, the instrument Micrometric/3FLEX 3500 was utilized. The instrument used gas sorption techniques to measure the surface area and pore size [15]. The textural characteristics were determined by performing N<sub>2</sub> adsorption isotherms at 77K. The BET equation was used to get the specific surface area (SBET), the Dubinin-Radushkevich equation was used to calculate the volume of micropores, and the Barrett-Joyner-Halenda (BJH) method was used to calculate the pore size distribution. Similar method was reported by [15]-[17]. To remove any moisture present in the sample, the two carbon samples of palm kernel shell biochar (PKS) and xerogel were degassed at 120 °C under a continuous nitrogen flow of 10 L/min for 24 hours prior to analysis which is similar to the parameters used by [1].

### **Scanned electron microscopy (SEM)**

The purpose of SEM is to identify the surface morphology xerogel using a scanning electron microscope with a 5k accelerating voltage. According to ASTM E986-04, the range of magnification is 1000-50000 X. Before proceeding with the SEM analysis, all the xerogel biochar samples were coated in a gold film to remove any residual ions on the sample. Based on the study by [12] stated that many studies related to silica aerogel/xerogel utilize two different approaches to morphology which are sponge-like and pearl-like observation. In previous work by [12], it was found that typical xerogel properties are porous materials with a percentage of 80%-90% porosity. The porosity of silica network is in the form of three-dimensional and their main classes for porous materials are microporous, mesoporous, and microporous.

## **Results and Discussion**

### **Chemical properties**

FTIR spectrums were used to identify the existence and the changes of functional groups from palm kernel shell (PKS) biochar to a synthesized xerogel. Figure 5 shows the FTIR spectrum of (a) palm kernel shell (PKS) biochar and (b) xerogel biochar for comparison. Figures 5a and 5b have shown peaks in the O-H stretching region. The spectrum shows broad characteristic peaks at 3356.82 cm<sup>-1</sup> for PKS biochar and 3333.76 cm<sup>-1</sup> for xerogel biochar, which indicates the presence of O-H stretching. The same results were shown in [8] which the same peak was recognized to be the stretching functional group of a hydrogen-bonded hydroxyl group (O-H). This is indicative of the presence of alcohols and due to H<sub>2</sub>O absorption on the PKS biochar and

xerogel surface. Stretching vibration of C-H with wavelength 2942.51  $\text{cm}^{-1}$  for PKS biochar and 2917.64 to 2849.73  $\text{cm}^{-1}$  for xerogel was observed. As reported by Ma et al, [18], the band with a width of 2919  $\text{cm}^{-1}$  was designated the stretching vibration of the C-H bond of the alkane and aldehyde group. The presence of functional group C=C stretching on 1637  $\text{cm}^{-1}$  for PKS biochar, and 1616.98  $\text{cm}^{-1}$  was shown. According to [18], peaks around 1690-1450  $\text{cm}^{-1}$  indicated the presence of aromatics compounds. Holocellulose and lignin are hydrocarbon polymers consisting of aliphatics and aromatic structures [15]. This shows that the formation of xerogel biochar does not destroy the lignin compound which is important to the structure of xerogel biochar. A similar aromatic ester is found at a bending vibration of 1314.05  $\text{cm}^{-1}$  in Figure 5b.

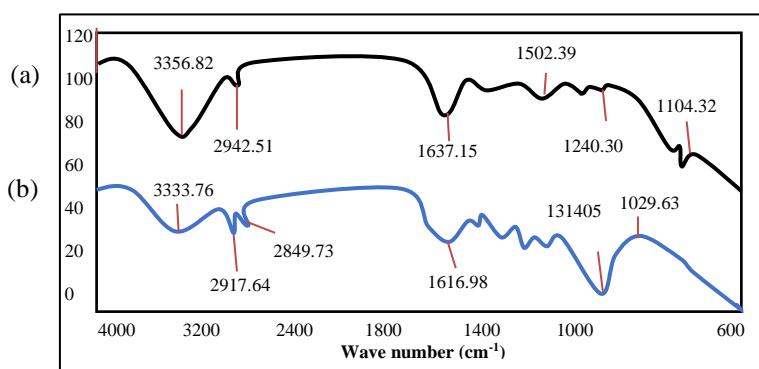


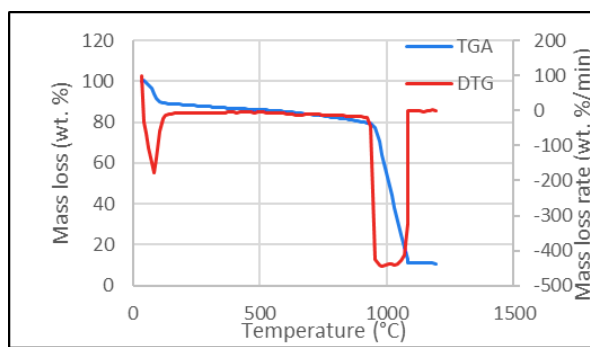
Figure 4: FTIR graph analysis'; (a) palm kernel shell biochar, and (b) xerogel components Biochar

Volatiles were identified in Figure 4a at the bending vibration around 1466  $\text{cm}^{-1}$  representing the existence of the C-C and C-H (alkane) groups. The bending vibration of xerogel begins to change its spectrum around 1100  $\text{cm}^{-1}$ . This is because of the addition of Sodium alginate as a copolymer and Calcium Carbonate as a cross-linker in the polymerization process. A peak at 1029  $\text{cm}^{-1}$  shows the existence of the S=O group in xerogel.

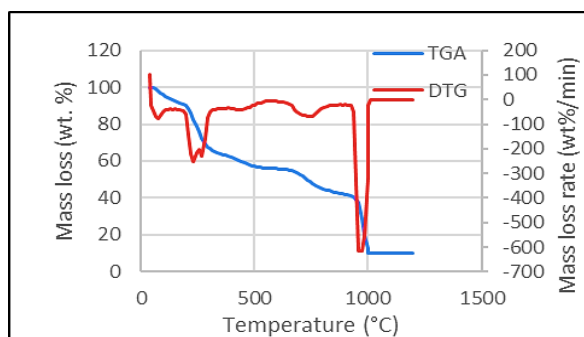
### TGA analysis

Thermogravimetric Analysis (TGA) is done following the ASTM standard method D5142-02a to study the element content and the thermal stability of the extracted xerogel biochar. TGA curve shows that the pyrolysis of studied xerogel and palm kernel shell (PKS) biochar is divided into four stages where it depicts the element content of moisture (%), volatile matter (%), ash (%), and fixed carbon (%) content. The TGA curves for xerogel biochar and palm kernel shell (PKS) biochar are shown in Figure 6a and Figure 6b, respectively.

Water, cellulose, hemicellulose, and lignin are the four primary components of the biochar source which in this case is palm kernel shell (PKS) [19]. The thermogravimetric analysis is plotted by pairing thermogravimetric and derivative thermogravimetric (TG-DTG) curves to show the relationship between the mass change of TGA and the differentiation of TGA with time.



(a)



(b)

Figure 5: TG-DTG curves at a heating rate of 20 °C/min; (a) PKS biochar, and (b) Xerogel biochar

Figure 5a and Figure 6b also show the TG (primary y-axis) and DTG (secondary y-axis) curves for the studied xerogel and palm kernel biochar. Figure 6a shows the TGA curve of palm kernel shell (PKS) biochar where the first stage is the mass loss of 10.9% (2.2 mg) up to 144.55 °C due to the removal of moisture from the PKS biochar sample. Meanwhile, Figure 6b shows a mass loss of 7.03% (1.4 mg) was found in the first step of the TGA curve of xerogel biochar at around 146.64°. This mass loss is mainly attributed to the physical adsorption of water in the xerogel at the first step of the TGA curve. The sample mass slightly declined up to about 33 min with a mass loss

of 1.93 mg (9.64%) and left a residue of 15.88 mg (79.4%) for PKS biochar. In the case of xerogel biochar, the temperature around (200 °C to 400 °C) is mostly connected to the decomposition of volatile materials from hydrogel polymerization, such as cellulose, hemicelluloses, and some sodium alginate co-polymer [7]. The mass loss at the second step is 52.1% (10.42 mg). A significant mass loss in the xerogel sample is higher than PKS biochar in step 2 due to the chemically bound water from the weight reduction that was attributed to chemically bonded water from the sol-gel manufacturing technique [8]. Moreover, the volatile component of a sample depends on the lignin and cellulosic content of biomass and the pyrolysis temperature [15]. According to [16], after 20 minutes at around this temperature, the weight loss is often less than 2 g/min, indicating that no noticeable oxygen is entering the Standard Thermogravimetric Analysis. After switching the atmosphere to oxidizing atmosphere combustion of air at 950 °C, a remarkable mass loss of 68.5% (13.7 mg) is shown at 938.16 °C and a mass loss of 30.96% (6.2 mg) is shown at between 950-1000 °C for PKS biochar and xerogel biochar, respectively. The final peak at 950 °C represents carbon thermal breakdown, and the remaining curve represents ash content. This was a significant mass loss which might be due to the elimination of volatile matters and lesser stable constituents of PKS due to thermal degradation [3]. Complete degradation of xerogel biochar is recorded at 1189.97 °C. The three regions are in an agreement with related literature as reported in [5], [7] and [16]. It can be concluded from the TGA analysis that xerogel biochar is stabilized due to no further decompositions is occurred. Therefore, it can be used as an adsorbent up to 1000 °C. The proximate analysis results were provided in Table 2. It can be observed that the moisture content was decreasing from PKS biochar of 10.9% and became xerogel biochar of 7.03%. After the polymerization process, the volatile matter increased significantly from the PKS biochar of 9.64% and became 52.1%. In addition, PKS biochar had higher carbon content at 68.5 % compared to xerogel at 30.96%. The reason is that PKS biochar has higher carbonaceous substances and oxidized some amount of carbon in the biochar [7]. Finally, the ash content of PKS biochar was slightly higher at 10.87 % compared to xerogel with only 9.86%.

Table 2: Proximate analysis of PKS biochar and xerogel biochar

Material	Moisture content (%)	Volatile content (%)	Carbon content (%)	Ash content (%)
PKS Biochar	10.9	9.64	68.5	10.87
Xerogel Biochar	7.03	52.1	30.96	9.86

### **X-Ray diffraction analysis**

The XRD pattern of xerogel and palm kernel shell (PKS) biochar is shown in Figure 6. A typical broad peak at around  $2\theta = 20-30^\circ$  for both xerogel and PKS

biochar is observed. The observed pattern is an indication of the amorphous nature of xerogel. According to [17], this is also attributed to the presence of disordered cristobalite. A similar result was identified by other researchers namely, [8], [13] and [18]. It can be observed that an additional peak around  $2\theta = 40^\circ$  is formed for the xerogel XRD pattern, which is resulting from the addition of sodium alginate.

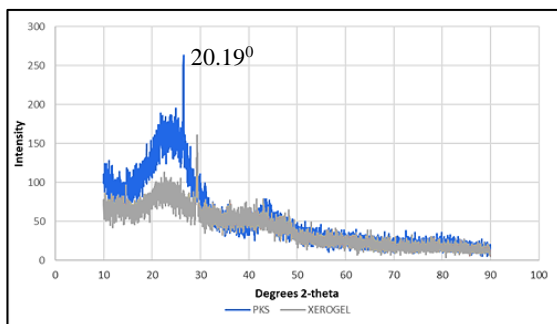


Figure 6: The XRD graph for xerogel and palm kernel shell (PKS) biochar

### Surface area and pore volume

Nitrogen adsorption isotherms, as the amount of  $N_2$  adsorbed as a function of relative pressure at  $-196^\circ C$ , are shown in Figure 7a and 7b. Following IUPAC classification, the isotherms type IV and with a hysteresis loop is associated with mesoporous materials [8], [19]. To determine more information on the porous structure of palm kernel shell (PKS) biochar and xerogel, Brunauer-Emmett and Teller (BET), Barrett-Joyner-Halenda (BJH) and t-plot analysis were used.

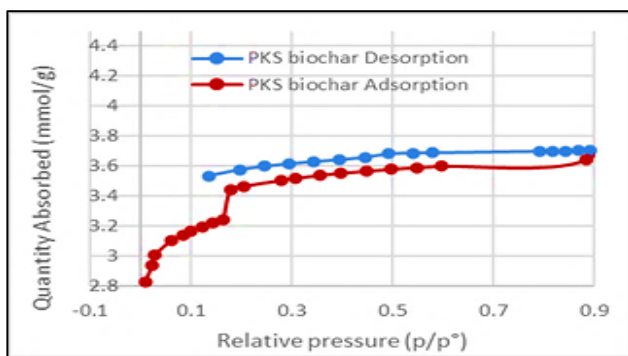


Figure 7 (a): BET isotherm plot for PKS biochar

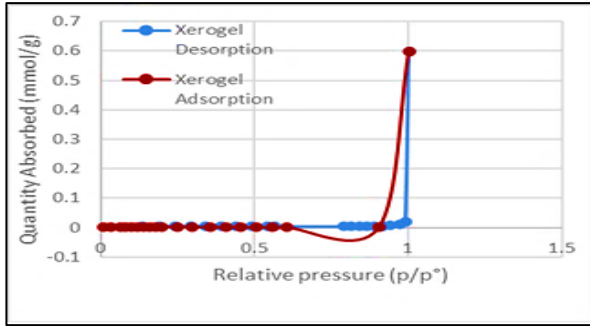


Figure 7 (b): BET isotherm plot for xerogel biochar

The isotherm plot in Figure 7a for PKS biochar shows typical Type IV isotherms, typical of mesoporous materials [20]. Meanwhile, the isotherm plot in Figure 7b is clustered as type III where a similar isotherm for xerogel was reported by [16]. Table 3 shows the result summary for textural characteristics such as BET surface area, the total micropore volume, and average pore diameter and pore width for PKS biochar and xerogel biochar, respectively. The BET surface area, SBET of xerogel was found to be 0.26 m<sup>2</sup>/g which is relatively low compared to PKS biochar. It is convenient to classify pores according to their diameters in the context of physisorption where pores with widths exceeding about 50 nm (0.05 μm) are called macropores, pores of widths between 2 nm and 50 nm are called mesopores and pore with widths not exceeding about 2 nm are called micropores [21]. Therefore, xerogel exhibits micropore characteristics as the pore width is 1.5 nm which is lesser than 2 nm. On contrary, PKS biochar is considered as mesopores as the pore width is 2.3 (>2nm).

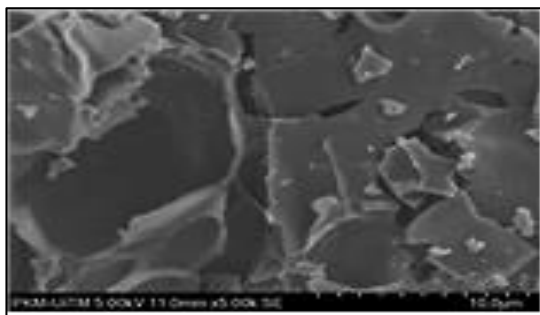
Table 3: BET surface area and pore size distribution results

Material	S <sub>BET</sub> (m <sup>2</sup> .g <sup>-1</sup> )	V <sub>micro</sub> (cm <sup>3</sup> .g <sup>-1</sup> )	Average pore diameter (m <sup>2</sup> .g <sup>-1</sup> )	Pore width (nm)
PKS biochar	289.7954	0.086725	1.8	2.3
Xerogel	0.2686	0.000063	9.3	1.5

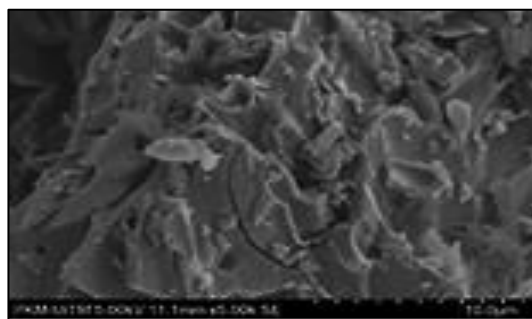
### Surface morphology

The SEM micrograph is produced for xerogel, palm kernel shell (PKS) biochar and activated carbon at x5000 magnification in 10 μm size. As shown in Figures 8a and 8b, the xerogel and palm kernel shell (PKS) biochar samples have a highly irregular, fibrous surface structure, with little regular texturing. The structure of the xerogel had a highly complex network of pores, and rough

surfaces as opposed to the PKS biochar surface. This can be confirmed with BET analysis which shows a very small pore diameter size. The SEM pictures of xerogel and PKS biochar also show an alignment of honeycomb-like groups of pores, which is most likely the carbonaceous skeleton from the capillary structure of botanical origin [22].



(a)



(b)

Figure 8: SEM image of; (a) palm kernel shell (PKS) biochar, and (b) xerogel

## **Conclusion**

Palm kernel shell (PKS) biochar has been used as the raw material due to the high amount of carbon content. To combat environmental pollution, green alternatives are in search for decades. Therefore, the study of xerogel produced from palm kernel shell (PKS) biochar has been done in this research. From the FTIR spectrum, it has been shown that xerogel depicts changes in various functional groups from palm kernel shell (PKS) biochar. The TGA analysis revealed that xerogel biochar can be utilized as an adsorbent up to 1000 °C.

An amorphous phase was identified by XRD analysis for both xerogel, and palm kernel shell (PKS) biochar was a successful finding as amorphous materials are widely used in the adsorption industry. The BET analysis revealed the pore width to be 1.5 nm which is a microporous material that is related to the SEM images. The SEM images show that xerogel appeared to have a highly complex pore size, porous structure and irregular surface because of its small pore size which matched with a typical xerogel as an adsorbent. In the future, xerogel biochar will be widely used in adsorption industries, and a regeneration study will be conducted to increase the ability to achieve an adsorbent that does not harm the environment and can easily be generated for long-term usage. As a result, it is critical that these characterizations be carried out before they are experimentally applied to environmental systems.

## **Acknowledgment**

The authors would like to thank the College of Engineering, Universiti Teknologi MARA (UiTM) for the financial support. The research was conducted at the School of Chemical Engineering, UiTM under the support of a university industrial collaboration (UIC) grant (100-TNCPI/PRI 16/6/2 (024/2022)).

## **References**

- [1] N. F. Ahmad, A. B. Alias, N. Talib, Z. A. Rashid, and W. A. W. A. K. Ghani, "Characteristics of Rice Husk Biochar Blended with Coal Fly Ash for Potential Sorption Material," *Malaysian J. Anal. Sci.*, vol. 22, no. 2, pp. 326–332, 2018.
- [2] N. H. Meri, A. B. Alias, N. Talib, Z. A. Rashid, W. A. Wan, and A. Karim Ghani, "Effect of Chemical Washing Pre-treatment of Empty Fruit Bunch (EFB) biochar on Characterization of Hydrogel Biochar composite as Bioadsorbent," *IOP Conf. Ser. Mater. Sci. Eng.*, vol. 358, no. 1, 2018, doi: 10.1088/1757-899X/358/1/012018.
- [3] S. A. S. N. Fadzli, S. Roslind, and Z. Firuz, "Sol-gel synthesis and preliminary characterizations of novel silica hybrid xerogels," *Key Eng. Mater.*, vol. 594–595, no. January 2017, pp. 1009–1014, 2014, doi: 10.4028/www.scientific.net/KEM.594-595.1009.
- [4] M. Kumari and A. K. Saroha, "Synthesis and characterization of carbon xerogel based iron catalyst for use in wet air oxidation of aqueous solution containing 2, 4, 6-trichlorophenol," *J. Environ. Chem. Eng.*, vol. 7, no. 3, 2019, doi: 10.1016/j.jece.2019.103121.

- [5] S. Groult, S. Buwalda, and T. Budtova, "Pectin hydrogels, aerogels, cryogels and xerogels: Influence of drying on structural and release properties," *Eur. Polym. J.*, vol. 149, no. February, 2021, doi: 10.1016/j.eurpolymj.2021.110386.
- [6] N. M. F. M. Yasin, N. H. Meri, N. Talib, W. A. W. A. K. Ghani, Z. A. Rashid, and A. B. Alias, "Breakthrough Analysis of Empty Fruit Bunch-Based Hydrogel Biochar Composite (EFB-HBC) for Hydrogen Sulphide (H<sub>2</sub>S) Adsorption Study Removal," vol. 200, no. ICoST, pp. 216–225, 2021, doi: 10.2991/aer.k.201229.030.
- [7] P. E. Imoisili, K. O. Ukoba, and T. C. Jen, "Green technology extraction and characterisation of silica nanoparticles from palm kernel shell ash via sol-gel," *J. Mater. Res. Technol.*, vol. 9, no. 1, pp. 307–313, 2020, doi: 10.1016/j.jmrt.2019.10.059.
- [8] Z. Wu, H. Joo, and K. Lee, "Kinetics and thermodynamics of the organic dye adsorption on the mesoporous hybrid xerogel," vol. 112, pp. 227–236, 2005, doi: 10.1016/j.cej.2005.07.011.
- [9] A. K. Thakur, R. Singh, R. T. Pallela, and V. Pundir, "Green adsorbents for the removal of heavy metals from Wastewater: A review," *Mater. Today, Proc.*, vol. 2021, p. 5, 2021, doi: 10.1016/j.matpr.2021.11.373.
- [10] O. D. Jayakumar and A. K. Tyagi, *Spintronic materials, synthesis, processing and applications. Functional Materials.*, pp. 193– 228., 2012, <http://dx.doi.org/10.1016/B978-0-12-385142-0.00005-2>.
- [11] Y. Hannachi, A. Hafidh, and S. Ayed, "Effectiveness of novel xerogels adsorbents for cadmium uptake from aqueous solution in batch and column modes: Synthesis, characterization, equilibrium, and mechanism analysis," *Chem. Eng. Res. Des.*, vol. 143, pp. 11–23, 2019, doi: 10.1016/j.cherd.2019.01.006.
- [12] G. G. Kaya and H. Deveci, "Synergistic effects of silica aerogels/xerogels on properties of polymer composites: A review," *J. Ind. Eng. Chem.*, vol. 89, pp. 13–27, 2020, doi: 10.1016/j.jiec.2020.05.019.
- [13] J. P. Paques, "Alginate Nanospheres Prepared by Internal or External Gelation with Nanoparticles" *Microncapsulation and Microspheres for Food Application.*, pp. 39- 55., 2015, <https://doi.org/10.1016/B978-0-12-800350-3.00004-2>.
- [14] P. E. Imoisili, K. O. Ukoba, and T. Jen, "Synthesis and characterization of amorphous mesoporous silica from palm kernel shell ash," *Boletín la Soc. Española Cerámica y Vidr.*, vol. 59, no. 4, pp. 159–164, 2019, doi: 10.1016/j.bsecev.2019.09.006.
- [15] N. F. Ahmad, A. B. Alias, N. Talib, Z. A. Rashid, and W. A. W. A. K. Ghani, "Characterization of upgraded hydrogel biochar from blended rice husk with coal fly ash," *AIP Conf. Proc.*, vol. 1901, pp. 1-7., 2017, doi: 10.1063/1.5010578.

- [16] L. Kocon et al., “Carbon aerogels, cryogels and xerogels: Influence of the drying method on the textural properties of porous carbon materials,” vol. 43, pp. 2481–2494, 2005, doi: 10.1016/j.carbon.2005.04.031.
- [17] S. A. C. Carabineiro, T. Thavorn-amornsri, M. F. R. Pereira, P. Serp, and J. L. Figueiredo, “Comparison between activated carbon, carbon xerogel and carbon nanotubes for the adsorption of the antibiotic ciprofloxacin,” *Catal. Today*, vol. 186, no. 1, pp. 29–34, 2011, doi: 10.1016/j.cattod.2011.08.020.
- [18] Z. Ma, D. Chen, J. Gu, B. Bao, and Q. Zhang, “Determination of pyrolysis characteristics and kinetics of palm kernel shell using TGA-FTIR and model-free integral methods,” *Energy Convers. Manag.*, vol. 89, pp. 251–259, 2015, doi: 10.1016/j.enconman.2014.09.074.
- [19] H. Bamdad, “A theoretical and experimental study on biochar as an adsorbent for removal of acid gases (CO<sub>2</sub> and H<sub>2</sub>S),” *Energy and Fuels*, vol. 32, pp. 11742–11748, 2018, <http://dx.doi.org/10.1021/acs.energyfuels.8b03056>.
- [20] S. Katarzyna, B. Pietro, F. Francesco, “Thermogravimetric analysis and kinetic study of poplar wood pyrolysis” *Applied Energy*, Vol. 97, pp. 491–497, 2012, <https://doi.org/10.1016/j.apenergy.2011.12.056>
- [21] C. Channoy, S. Maneewan, C. Punlek, and S. Chirarattananon, “Preparation and Characterization of Silica Gel from Bagasse Ash,” vol. 1145, pp. 44–48, 2018, doi: 10.4028/www.scientific.net/AMR.1145.44.
- [22] W. a W. Ab, K. Ghani, K. a Matori, and A. B. Alias, “Physical and Thermochemical Characterisation of Malaysian Biomass Ashes,” *Inst. Eng. Malaysia*, vol. 71, no. 3, pp. 9–18, 2010.